



On-line FTIR as a novel tool to monitor Fenton process behavior



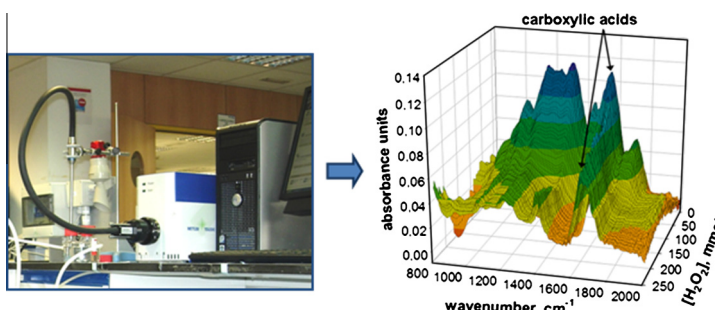
Noemí Merayo, Daphne Hermosilla*, Carlos Negro, Ángeles Blanco

Department of Chemical Engineering, Complutense University of Madrid, Facultad de Ciencias Químicas, Ciudad Universitaria s/n, 28040 Madrid, Spain

HIGHLIGHTS

- On-line FTIR is shown as a suitable alternative for real-time reaction control.
- FTIR was successfully applied to monitor the Fenton oxidation of model compounds.
- FTIR-based real-time control allowed the finest Fenton's process optimization.
- The proposed methodology saved much time for analyses monitoring Fenton processes.

GRAPHICAL ABSTRACT



ARTICLE INFO

Article history:

Received 30 March 2013
Received in revised form 7 July 2013
Accepted 27 July 2013
Available online 9 August 2013

Keywords:

Advanced oxidation processes
Fenton method
Fourier transform infrared spectroscopy
Treatment on-line monitoring
Phenol

ABSTRACT

The efficiency of advanced oxidation processes is usually optimized by measuring the evolution of some water quality parameters sampling aliquots at pre-selected time intervals, such as particular undesired contaminants contents, or the reduction of chemical oxygen demand and total organic carbon. Besides providing good information regarding overall treatment performance and dynamics, this methodology also implies large analytical time consumption, and does not offer the actual full sequence of compounds appearing and disappearing during oxidation. On-line Fourier transform infrared spectroscopy is herein reported as a very useful tool for this purpose. In particular, it was successfully applied to monitoring the Fenton's oxidation of three model compounds (phenol, acetic acid, and oxalic acid) performed in continuous, providing precise control of the effect of reagents over time. Hydroxylation reactions resulted in the formation of hydroquinone and catechol as the main aromatic by-products being generated along the oxidation of phenol by the Fenton process. All phenolic substances (phenol, hydroquinone, benzoquinone, and catechol) were totally removed along the reaction. Carboxylic acids (oxalic and acetic mainly) were significantly present as final by-products of the oxidation process, highlighting their oxyrecalcitrant behavior. On-line FTIR successfully enabled monitoring the Fenton process, and it provided a precise control of the effect of reagents along reaction time. Applications for a future on-line control of Fenton processes in industry may be developed in order to optimize the use of reagents and the potential combination with biological treatment stages; therefore reducing the operational cost of this advanced oxidation treatment.

© 2013 Elsevier B.V. All rights reserved.

1. Introduction

Advanced oxidation processes (AOPs) involving the *in situ* generation of highly reactive transitory species (e.g. H_2O_2 , OH^\cdot , O_3 , O_2^\cdot) are taking advantage when conventional wastewater treatment techniques become insufficient to treat biorefractory contaminants

[1–5]. Particularly, the method described by Fenton [6] is one of the most frequently used because it is generally more efficient, and implies a significant lower economical cost than other AOPs [2,5,7,8].

The Fenton process is based on the electron transfer between hydrogen peroxide (H_2O_2) and ferrous ion (Fe^{2+}), which acts as a homogenous catalyst, generating hydroxyl radicals (OH^\cdot) that can degrade organic compounds [9]. These highly reactive radicals initiate the oxidative destruction of organic substances (RH) present

* Corresponding author. Tel.: +34 91 394 4645; fax: +34 91 394 4243.
E-mail address: dhermosilla@quim.ucm.es (D. Hermosilla).

in wastewater by hydroxyl radical addition or hydrogen atom abstraction reactions [5]. Organic free radicals (R[•]) are formed as transient intermediates that are further oxidized by hydroxyl radical, hydrogen peroxide, oxygen, ferric iron, and other oxidative intermediates; finally yielding stable oxidized products [5].

The optimization and process control of Fenton treatment and other AOPs has usually been undertaken by measuring certain water quality parameters (e.g. undesired contaminants contents, chemical oxygen demand, and/or total organic carbon removal) at certain time intervals. In addition, several techniques have widely been applied to characterize the sequence of organic compounds that are produced during the oxidative treatment using this discrete sampling protocol, such as high-performance liquid chromatography (HPLC) [10–12], gas chromatography–mass spectrometry (GC–MS) [13,14], Fourier transform infrared spectroscopy (FTIR) [15,16], or different combinations of them, or with other analytic techniques (e.g. ultraviolet–visible spectrophotometry (UV–Vis), liquid chromatography–mass spectrometry (LC–MS), ion chromatography (IC), etc.) [17–21].

Particularly, FTIR has been previously applied to analyze the surface of catalysts and adsorbed substances along diverse AOPs treatments [22–25]. Gas samples have also been analyzed by FTIR to measure the generation of carbon dioxide (assimilable as mineralized carbon) in outlet gaseous streams of ozonation processes, which served as an indirect control parameter of the treatment [26]. In addition, FTIR has also been applied to control reactions in liquid samples identifying the compounds that are appearing and disappearing in the solution at preset time intervals [15,16]. All these methods enabling an indirect discrete control of the reaction involve great analytical time investment, and do not provide a full continuous characterization of the sequence of compounds that are produced in, or removed from the solution along the process. Furthermore, no reference for its on-line application has been reported to date.

On the other hand, membrane-introduction mass spectrometry (MIMS) has actually been applied to perform on-line measurements along photocatalytic processes [27]. Nevertheless, despite this methodology has been reported useful for monitoring these processes on-line, just volatile organic pollutants that are present in water can be effectively analyzed; whereas other highly polar substances could not be detected properly, such as some compounds that have been previously reported to be typically generated along the oxidation process of phenol [27].

Moreover, the current tendency of improving the combination of AOPs with biological technologies [28,29] would surely welcome the application of advanced analytical methods to optimize the efficiency of every treatment step considering the predominant bio- or oxi-degradable nature of by-products. Therefore, the main objective of this essay was developing a suitable methodology of on-line monitoring the evolution of the Fenton treatment of model organic compounds based on FTIR; which may ultimately allow the addition of reagents to be optimized, a further identification of the involved reactions, and the qualitative and quantitative determination of the by-products that are generated along the process.

2. Materials and methods

2.1. Material and analytical methods

All used chemicals were of analytical grade and supplied by PANREAC S.A. (Barcelona, Spain) and Sigma–Aldrich (Highland, USA). Solutions were prepared in ultrapure water and kept in dark until use. 0.1 N H₂SO₄ and 0.1 N NaOH were used to adjust the pH value of the solution along the process.

The concentration of each tested organic compound (16 mmol of phenol, 14 mmol of oxalic acid, and 12 mmol of acetic acid in a total volume of 100 mL) was considered in order to achieve a good monitoring resolution of the process in the ReactIR iC10 device. Phenol was chosen as a model compound to perform this essay because its degradation behavior by several AOPs (Fenton process included) has widely been described previously [30–34], so it would perfectly serve to evaluate the proposed methodology. In addition, oxalic and acetic acids were also chosen due to its oxy-recalcitrant nature [32].

All analyses were made according to the standard methods for the examination of water and wastewaters [35]. Chemical oxygen demand (COD) was measured by the colorimetric method at 600 nm using an Aquamate-spectrophotometer (Thermos Scientific AQA 091801, Waltham, USA); and hydrogen peroxide concentration was analyzed using the titanium–sulphate spectrophotometric method [36]. As residual hydrogen peroxide in the solution interferes with COD analysis, this interference was corrected fitting the relationship between COD and hydrogen peroxide content to a second order polynomial equation ($DQO(H_2O_2) = -0.000020 \cdot [H_2O_2]^2 + 0.393239 \cdot [H_2O_2]$; $R^2 = 99.92\%$; $p = 0.0001$) [37].

Total organic carbon (TOC) was measured by the combustion-infrared method using a TOC/TN analyzer multi N/C[®] 3100 (Analytik Jena AG, Jena, Germany) with catalytic oxidation on cerium oxide at 850 °C. The integration of the information provided by the evolution of both COD and TOC along the oxidation treatment was assessed by calculating the mean oxidation number of organic carbon ($MOC = 4 \cdot [1 - (COD/TOC)]$), considering both COD and TOC in molar units) [32].

Phenol and reaction intermediates were complementary measured by High Pressure Liquid Chromatography (Model L920, Varian, CA, USA) with diode array (PDA) detection. Acetonitrile–water (15%:85%), and (50%:50%) were used as the eluent for aromatics and carboxylic acids, respectively. Sample injections of 20 µL were separated on a C-18 column (Vidac 250 mm × 4.6 mm ID × 5 µm) at 30 °C. The target compounds were measured at the following wavelengths: hydroquinone (290 nm), benzoquinone (245 nm), catechol (280 nm), phenol (270 nm), acetic acid and oxalic acid (200 nm).

2.2. FTIR analytical device

ReactIR iC10 (Mettler-Toledo, Columbia, USA) is a real-time *in situ* reaction monitoring system, based on FTIR spectrometry, that is able to provide all the organic chemical species that are present in the solution as the reaction is being performed. The FTIR spectrometer uses a mercury–cadmium telluride (MCT) detector that is cooled by liquid nitrogen; and measurements are optically taken using a diamond-tipped probe with a 1 m long fibre-optic conduit. This system was purged using instrumental-grade air; therefore preventing water vapour from collecting inside the optics, which may obscure spectral data otherwise.

Data acquisition was performed from 2000 to 650 cm⁻¹ with an 8 cm⁻¹ nominal resolution. 256 scans were co-added for each spectrum. A background of pure water was carried out using the same resolution and scanning conditions of the trials before each spectral record. These water spectra were subtracted from each corresponding resulting on-line spectra.

Real-time component analyses were performed using ConciRT software (Mettler-Toledo, Columbia, USA), which applies the curve-resolution mathematical algorithm for grouping wavenumber values that change absorbance intensity in the same way. This software calculates the associated component spectrum and the relative concentration profile in terms of absorbance units for each group; and it re-analyzes and updates all spectra and concentra-

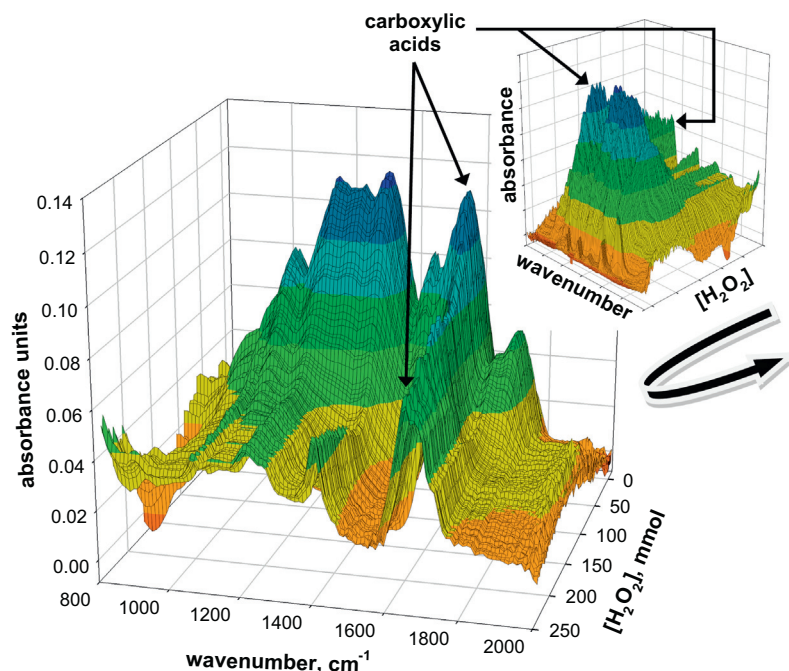


Fig. 1. Evolution of FTIR-spectra along a continuous hydrogen peroxide addition in the Fenton oxidation of phenol. The presence evolution of carboxylic acids is highlighted, and a turned around graph is also shown in small detail. (Reaction conditions: room temperature ($\approx 20\text{--}25\text{ }^{\circ}\text{C}$); $\text{pH} = 2.8 \pm 0.2$; 16 mmol phenol; $[\text{H}_2\text{O}_2]/\text{COD}_0 = 2.15$; $[\text{H}_2\text{O}_2]/[\text{Fe}^{2+}] = 37.5$).

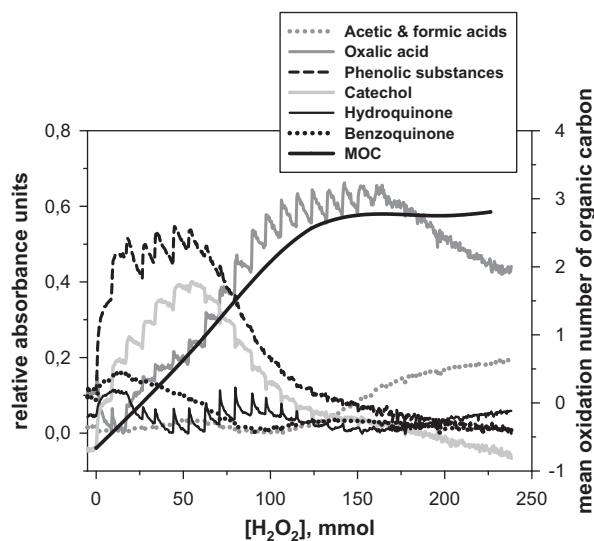


Fig. 2. Absorbance profiles for main by-products, and evolution of the MOC along a continuous hydrogen peroxide addition in the Fenton oxidation of phenol (Reaction conditions: room temperature ($\approx 20\text{--}25\text{ }^{\circ}\text{C}$); $\text{pH} = 2.8 \pm 0.2$; 16 mmol phenol; $[\text{H}_2\text{O}_2]/\text{COD}_0 = 2.15$; $[\text{H}_2\text{O}_2]/[\text{Fe}^{2+}] = 37.5$).

[31,33,40] and catechol (Fig. 2). On the other hand, resorcinol was not actually found along the Fenton oxidation of phenol. In fact, its formation would rather be implausible based upon the substitution rules of organic chemistry [33]; and it may anyhow occur in an about one thousand times lower frequency than the generation of catechol and hydroquinone [34].

The absorbance concentration profile of phenolic compounds logically increased as phenol was added to the solution; and it also grew again after the addition of H_2O_2 because other phenolic intermediate compounds of the reaction were newly formed (Fig. 2). During the reaction, this phenolic mix totally disappeared when

the concentration ratio between the added H_2O_2 and the initially supplied amount of phenol was close to 8, coinciding with previously reported results on the Fenton oxidation of phenol and nitrophenol, when a MOC value characteristic of the predominant presence of carboxylic acids ($\approx 2.5\text{--}3$) was kept more or less constant as the reaction progresses (Fig. 2) [32].

Achieving the total degradation of hydroquinone is of environmental concern due to its high toxicity, which is several orders of magnitude higher than the attributed to phenol itself [29]. On the other hand, catechol also resulted totally removed at the end of the reaction, as it has been clearly addressed by HPLC measurements. Nevertheless, catechol is highly biodegradable [41,42]; thus, it might be further treated by biological technologies, which are, in general, cheaper treatments than AOPs.

Furthermore, previous results reporting a significant much higher production of catechol than hydroquinone along the process were confirmed [33,34], as it results from comparing the concentration profiles of both compounds in Fig. 2. In fact, the production of catechol resulted a 100% higher than the measured for quinones by HPLC. In short, catechol and hydroquinone were initially formed as phenol disappeared; and then, they began to be gradually degraded competing with their own further formation as phenol was still being oxidized.

In addition, phenol decreased its concentration in the solution faster than the other newly generated phenolic intermediates (hydroquinone, benzoquinone, and catechol) of the reaction (comparing Figs. 2 and 3); which is also in accordance to previous scientific reports [32–34]. Only a 4% of phenol remained after adding a ratio of H_2O_2 to phenol of 3.9; results that were further confirmed by HPLC analyses.

At this point, the removal of COD was higher than 50%, and it did not show further lineal progress (Fig. 3). Finally, phenol resulted totally degraded when the aggregated concentration of H_2O_2 reached 5.6 times the initial amount of added phenol, and the reduction of the COD was close to a 75%; showing a further asymptotic evolution because of the growing presence of carboxylic acids, which are more difficult to oxidize. Hereafter, the mix

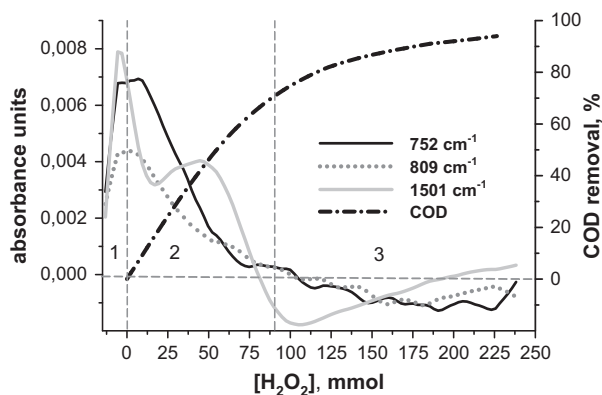


Fig. 3. Smooth absorbance concentration profiles of phenol, and evolution of the removal of the COD along the Fenton oxidation of phenol considering all its three typical detection wavenumbers (752, 809, and 1501 cm^{-1}). Note: 1 = addition of reagents; 2 = progressive removal of phenol; 3 = after the total removal of phenol.

of phenolic compounds remaining in the solution was mainly made up by hydroquinone and catechol (Fig. 2), which absorbance concentration profile quickly decreased until the ratio between the total added H_2O_2 and the initial amount of phenol was close to 6.5. Then, its abatement thereafter progressed smooth, and its total degradation was finally achieved when this ratio arrived to about 8, as confirmed by HPLC determinations.

Some carboxylic acids remained in the solution at the end of the process as the main persistent by-products of the oxidation treatment of phenol (Fig. 1); although they are also considered highly biodegradable and might be further treated by biological processes [41,42]. Oxalic, acetic, and formic acids were identified as the resultant products of an acid formation stage within the process. Its presence and persistence was also confirmed by HPLC measurement, and MOC and COD behavior assessment (Figs. 2 and 3), as just stated before. That is, its presence resulted constant after the ratio of total added H_2O_2 to the initial amount of phenol reached a value close to 8, which was accurately measured by HPLC; and also confirmed by a nonfurther change of MOC from characteristic values previously addressed for carboxylic acids mix [32], although COD was still slightly being removed (Figs. 2 and 3).

In short, carboxylic acids were probably formed by ring-opening reactions that take place within degradation stages of some aromatic intermediate products of the reaction [32,33]. Whilst the presence of oxalic acid was detected from almost the beginning of the reaction (Fig. 2), when the ratio of total added $[\text{H}_2\text{O}_2]$ to the initial concentration of phenol was just 1.8; acetic and formic acids presence was noticed in the solution when this ratio reached 6.25, suggesting that these two carboxylic acids may be generated by the degradation of some other intermediate reaction by-products.

All these carboxylic acids that are inevitably formed during the oxidative degradation of phenol are more or less recalcitrant to its further Fenton advanced oxidation treatment [1,16]; so they will hereafter be considered as oxyrecalcitrant compounds [32]. In fact, this limited capacity to degrade carboxylic acids is one of the main drawbacks for achieving the total mineralization of phenol by Fenton's reagent [32,33]. Therefore, the main objective of AOPs based treatment steps might be defined as controlling the process until a maximum biodegradability threshold is achieved in order to combine this treatment with a cheaper posterior biological stage [43].

In summary, a final 94% reduction of the COD was achieved (Fig. 3), which is even higher than previously reported results [30,32]. The continuous addition of H_2O_2 , which has previously been proved to enhance the removal of COD in comparison to batch mode [37], as well as the steady thorough control of the reaction conditions that was performed, have surely served well to achieve this very successful result. The 6% remaining COD was held

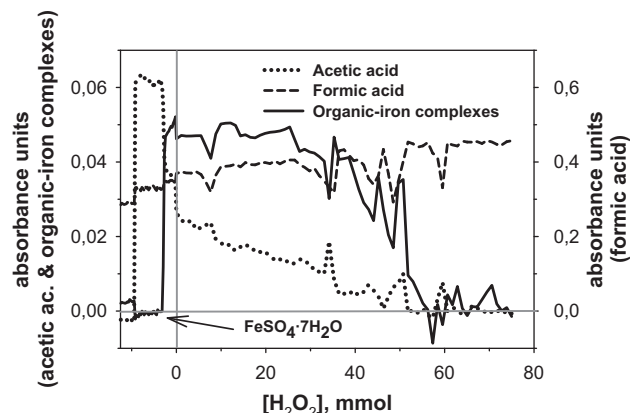


Fig. 4. Concentration profiles of acetic acid, formic acid and organic-iron complexes during the degradation of acetic acid by Fenton's reagent. (Reaction conditions: 12 mmol acetic acid, $\text{pH} = 2.8 \pm 0.2$, $[\text{H}_2\text{O}_2]/[\text{Fe}^{2+}] = 37.5$).

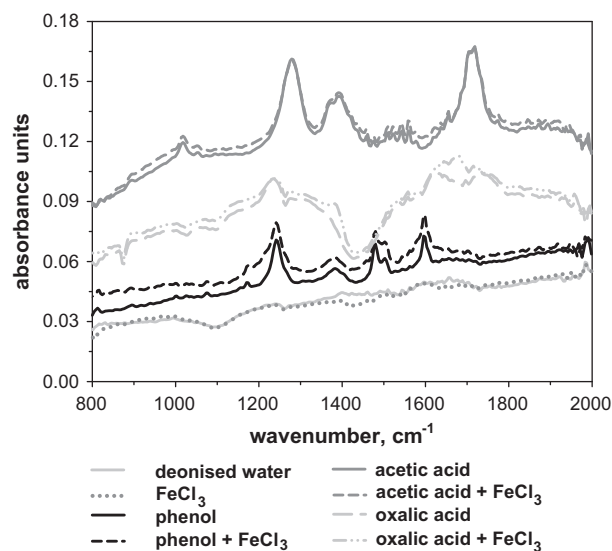


Fig. 5. FTIR spectra resulting for deionised water, phenol, acetic acid, and oxalic acid with and without the presence of ferric chloride trihydrate.

by the remaining mix of oxyrecalcitrant by-products, oxalic and other carboxylic acids, mainly.

3.2. Fenton treatment of acetic acid

When trying to oxidize acetic acid by Fenton's reagent, the initial addition of $\text{FeSO}_4 \cdot 7\text{H}_2\text{O}$ resulted in a colorless solution because the high production of a complex that is formed between acetic acid and ferrous iron drastically reduced the presence of both compounds in the solution (Fig. 4). As H_2O_2 was thereafter added, the concentration of this complex began to decrease, and the solution turned to an orange-reddish color as ferric ion was generated [38], which further induced the formation of an acetic acid–ferric iron complex. The formation of this complex is stronger than the acetic acid–ferrous iron one [32], but it was not detected by FTIR in the spectral region under study (Fig. 5). Nevertheless, the clearly noticed orange color of the solution, and the very limited figures of COD reduction, clearly suggest the presence of this ferric–acetic acid complex, as it has previously been reported [32].

The reaction may be considered finished when the ratio between the added concentration of H_2O_2 and the initial amount of supplied acetic acid reached 4.8. At this moment, the organic-fer-

rous iron complex disappeared because there was not any available Fe^{2+} to form more OH^\cdot that might have further continued the oxidation process, and the acetic acid–ferric iron complex (not visible to FTIR) and formic acid (Fig. 5) remained in the solution as the final result of the attempted degradation of acetic acid by the Fenton's reagent [44,45]. Final COD reduction figures were just about a 9% due to the above mentioned oxyrecalcitrant nature of this type of chemicals. In fact, these poor treatment results fully agree with other previously reported ones [32].

3.3. Fenton oxidation of oxalic acid

A constant weak green–yellow color predominated in the solution along the treatment of oxalic acid by Fenton's reagent; even after H_2O_2 was added. Therefore, ferrous to ferric ion oxidation was occurring at a very low pace; being oxalic acid itself contributing to reduce ferric back to ferrous [38]. This process partially slowed the oxidative process down because some H_2O_2 was being wasted on oxidizing ferrous iron back to ferric one.

In short, Fenton oxidation did not produce any degradation of oxalic acid (Fig. 6). In fact, great Fe^{2+} losses have previously been attributed to the formation of a strong oxalic–ferrous complex, which consequently hinders the oxidation process to progress [32]. Although this oxalic–ferrous complex was not detected by the FTIR probe, probably due to its very close likeness to other oxalic compounds, the oxidation process resulted similarly hindered.

In fact, the absorbance concentration profile of oxalic acid did not show any change after increasing the addition of H_2O_2 (Fig. 6); although it significantly decreased previously, just after

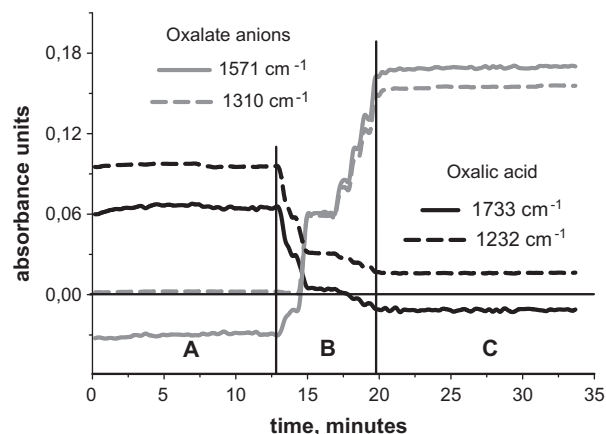


Fig. 7. Absorbance concentration profiles for characteristic wavenumber values of oxalic acid (1733 and 1232 cm^{-1}) and its anion (1571 and 1310 cm^{-1}) considering the following pH turns: (A) natural pH of an oxalic acid solution, (B) 40% NaOH addition to increase pH, and (C) pH values at which oxalic forms are stabilized (>9.0).

adjusting the pH (adding 40% NaOH), because oxalic acid and oxalate anion contents depend on the pH value of the solution [46]. That is, oxalate anion was formed as pH increased, as it is detailed in Fig. 7. Whereas the characteristic wavenumber peaks of oxalic acid (1733 and 1232 cm^{-1}) gradually decreased during the addition of 40% NaOH until its content stabilized at a very constant final value [46]; those typical peaks of oxalic anion (1571 and

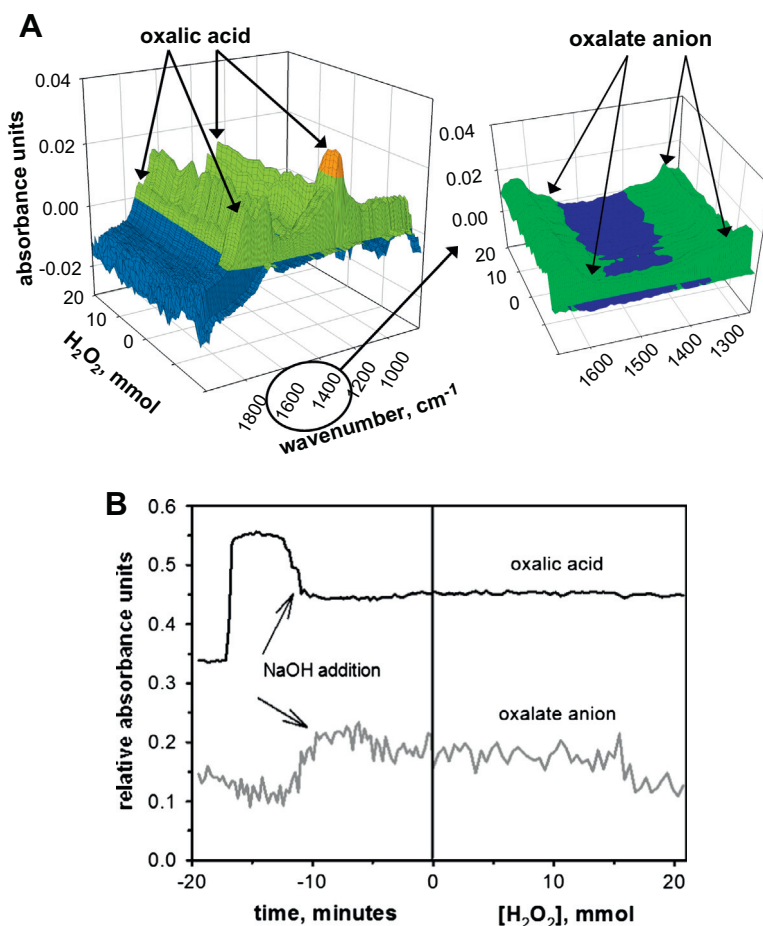


Fig. 6. Evolution of FTIR spectra in the span ranging from 2000 to 800 cm^{-1} (A), and concentration profiles of oxalic acid and oxalate (B) along the Fenton oxidation of oxalic acid. (Reaction conditions: 14 mmol oxalic acid, $\text{pH} = 2.8 \pm 0.2$, $[\text{H}_2\text{O}_2]/[\text{Fe}^{2+}] = 37.5$).

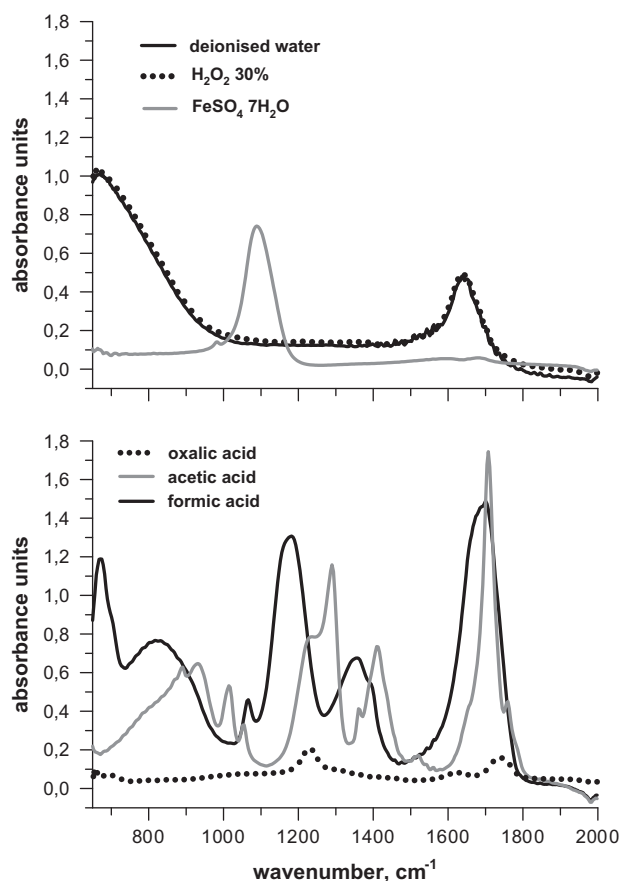


Fig. A.1. FTIR spectra of main inorganic and aliphatic compounds that are used and may be produced in the oxidation of phenol by the Fenton process.

1310 cm^{-1}) showed up, and correspondingly increased its absorbance record, after NaOH was added, until its content reached a steady state as well [46].

Summing up, the total removal of the COD that was achieved in the treatment of oxalic acid by Fenton's reagent resulted lower than the 7%. This result totally meets previously reported results [31,32], which also suggested that it is the variation of pH, rather than the oxidative treatment itself, which is the responsible of this reduction of the COD. In fact, this slight percentage of COD removal was surely the result of the final precipitation of oxalic acid when pH was turned to 9 adding NaOH at the end of the reaction aiming to remove iron precipitating its hydroxides.

4. Conclusions

The above reported results clearly show that the effectiveness of an oxidation process may successfully be assessed by FTIR, implying a significant reduction of the time devoted for analyses in comparison to other methodologies. In addition, it has been shown that the results obtained by FTIR were in total agreement with those previously reported using chromatographic analyses. That is, aliphatic organic compounds were not easily degraded with this type of treatment, whereas phenol resulted totally removed.

The quality and quantity of reaction intermediates that were produced during the oxidative degradation of phenol were fully assessed, and the mechanisms that were involved were also well observed. Thanks to receiving real-time information, this procedure allowed a precise control of the effects of reagents on the treated substances, which furthermore enabled optimizing the quantities

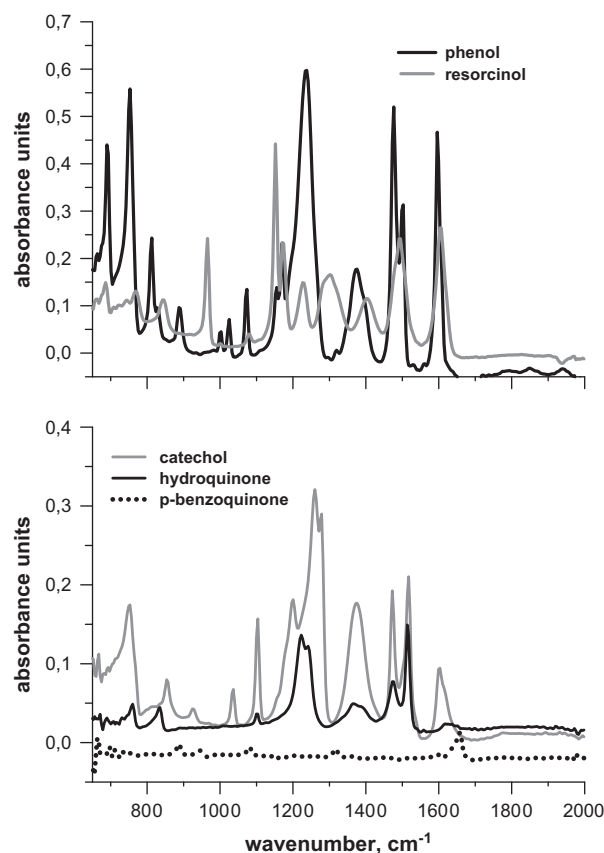


Fig. A.2. FTIR spectra of main aromatic chemicals that may be produced in the oxidation of phenol by the Fenton process.

of reagents required in the process. This may further enable the successful optimization of the treatment combination of AOPs with biological technologies, as the reaction moment where oxyrecalcitrant (but biodegradable) substances were mainly present in the solution was clearly identified.

Acknowledgements

This research was developed in the frame of the Projects "AQUAFIT4USE" (211534), funded by the European Union; "AGUA Y ENERGÍA" (CTM2008-06886-C02-01), and "OXIPAPEL" (CIT-310000-2008-15), both funded by the Ministry of Science and Innovation of Spain. N. Merayo's participation was sponsored by a Ph.D. Grant from the Ministry of Economy and Competitiveness of Spain.

Appendix A

Spectral characteristics of the chemical species produced along the Fenton oxidation treatment of phenol.

References

- [1] R.J. Bigda, Consider Fenton's chemistry for wastewater treatment, *Chem. Eng. Prog.* 91 (1995) 62–66.
- [2] S. Esplugas, J. Giménez, S. Contreras, E. Pascual, M. Rodríguez, Comparison of different advanced oxidation processes for phenol degradation, *Water Res.* 36 (2002) 1034–1042.
- [3] C. Comninellis, A. Kapalka, S. Malato, S.A. Parsons, I. Poullos, D. Mantzavinos, Advanced oxidation processes for water treatment: advances and trends for R&D, *J. Chem. Technol. Biotechnol.* 83 (2008) 769–776.

- [4] W.H. Glaze, J.W. Kang, D.H. Chapin, The chemistry of water-treatment processes involving ozone, hydrogen-peroxide and ultraviolet-radiation, *Ozone-Sci. Eng.* 9 (1987) 335–352.
- [5] C.P. Huang, C. Dong, Z. Tang, Advanced chemical oxidation: its present role and potential future in hazardous waste treatment, *Waste Manag.* 13 (1993) 361–377.
- [6] H.J.H. Fenton, Oxidation of tartaric acid in presence of iron, *J. Chem. Soc.* 65 (1894) 899–910.
- [7] F.J. Rivas, F.J. Beltrán, F. Carvalho, B. Acedo, O. Gimeno, Stabilized leachates: sequential coagulation-flocculation plus chemical oxidation process, *J. Hazard. Mater.* 116 (2004) 95–102.
- [8] W.Z. Tang, *Physicochemical Treatment of Hazardous Wastes*, Lewis Publishers, Boca Raton, FL, 2004.
- [9] F. Harber, J.J. Weiss, The catalytic decomposition of hydrogen peroxide by iron salts, *J. Am. Chem. Soc.* 45 (1934) 338–351.
- [10] J. Dzenkel, J. Theurich, D.W. Bahnemann, Formation of nitroaromatic compounds in advanced oxidation processes: photolysis versus photocatalysis, *Environ. Sci. Technol.* 33 (1999) 294–300.
- [11] K. Vinodgopal, J. Peller, Hydroxyl radical-mediated advanced oxidation processes for textile dyes: a comparison of the radiolytic and sonolytic degradation of the monoazo dye Acid Orange 7, *Res. Chem. Intermed.* 29 (3) (2003) 307–316.
- [12] H. Wang, J. Wang, Electrochemical degradation of 2,4-dichlorophenol on a palladium modified gas-diffusion electrode, *Electrochim. Acta* 53 (2008) 6402–6409.
- [13] J. Poerschmann, U. Trommler, Pathways of advanced oxidation of phenol by Fenton's reagent—identification of oxidative coupling intermediates by extractive acetylation, *J. Chromatogr. A* 1216 (2009) 5570–5579.
- [14] C. Justino, A.G. Marques, K.R. Duarte, A.C. Duarte, R. Pereira, T. Rocha-Santos, A.C. Freitas, Degradation of phenols in olive oil mill wastewater by biological, enzymatic, and photo-Fenton oxidation, *Environ. Sci. Pollut. Res.* 17 (2010) 650–656.
- [15] J. Araña, E. Tello Rendón, J.M. Doña Rodríguez, J.A. Herrera Medián, O. González Díaz, J. Pérez Peña, Highly concentrated phenolic wastewater treatment by the photo-Fenton reaction, mechanism study by FTIR-ATR, *Chemosphere* 44 (2001) 1017–1023.
- [16] O. Abbas, C. Rebufa, N. Dupuy, J. Kister, FTIR—multivariate curve resolution monitoring of photo-Fenton degradation of phenolic aqueous solutions. Comparison with HPLC as a reference method, *Talanta* 77 (2008) 200–209.
- [17] I. Udrea, C. Bradu, Ozonation of substituted phenols in aqueous solutions over CuO–Al₂O₃ catalyst, *Ozone-Sci. Eng.* 25 (2003) 335–343.
- [18] L. Carlos, D. Fabbri, A.L. Capparelli, A. Bianco Prevot, E. Pramauro, F.S. García Einschlag, Intermediate distributions and primary yields of phenolic products in nitrobenzene degradation by Fenton's reagent, *Chemosphere* 72 (2008) 952–958.
- [19] L. Carlos, D. Fabbri, A.L. Capparelli, A. Bianco Prevot, E. Pramauro, F.S. García Einschlag, Effect of simulated solar light on the autocatalytic degradation of nitrobenzene using Fe³⁺ and hydrogen peroxide, *J. Photochem. Photobiol. A: Chem.* 201 (2009) 32–38.
- [20] L.G. Devi, K.S.A. Raju, S.G. Kumar, Photodegradation of methyl red by advanced and homogeneous photo-Fenton's processes: A comparative study and kinetic approach, *J. Environ. Monit.* 11 (7) (2009) 1397–1404.
- [21] B. Kayan, B. Gözmen, M. Demirel, A.M. Gizir, Degradation of acid red 97 dye in aqueous medium using wet oxidation and electro-Fenton techniques, *J. Hazard. Mater.* 177 (2010) 95–102.
- [22] L. Palmisano, M. Schiavello, A. Sclafani, G. Martra, E. Borello, S. Coluccia, Photocatalytic oxidation of phenol on TiO₂ powders. A Fourier transform infrared study, *Appl. Catal. B* 3 (1994) 117–132.
- [23] M.B. Sayed, ¹H-NMR, UV-visible, and FT-IR spectral analyses for the conflicting impacts of proton mobility and H-bonding association on the mesomeric structure in azopyrogallol, catechol, resorcinol, quinol, and phenol derivatives of melamine, *Ind. Eng. Chem. Res.* 43 (2004) 4822–4826.
- [24] P.Z. Araujo, C.B. Mendive, L.A. García Rodenas, P.J. Morando, A.E. Regazzoni, M.A. Blesa, D. Bahnemann, FT-IR-ATR as a tool to probe photocatalytic interfaces, *Colloids Surf. A Physicochem. Eng. Asp.* 265 (2005) 73–80.
- [25] S. Horikoshi, T. Miura, M. Kajitani, H. Hidaka, N. Serpone, A FT-IR (DRIFT) study of the influence of halogen substituents on the TiO₂-assisted photooxidation of phenol and *p*-halophenols under weak room light irradiance, *J. Photochem. Photobiol. A: Chem.* 194 (2008) 189–199.
- [26] S.A. Carr, R.B. Baird, Mineralization as a mechanism for TOC removal: study of ozone/ozone-peroxide oxidation using FT-IR *Water Res.* 34 (16) (2000) 4036–4048.
- [27] R.F.P. Nogueira, R.M. Alberici, M.A. Mendes, W.F. Jardim, M.N. Eberlin, Photocatalytic degradation of phenol and trichloroethylene: on-line and real-time monitoring via membrane introduction mass spectrometry, *Ind. Eng. Chem. Res.* 38 (1999) 1754–1758.
- [28] D. Mantzavinos, E. Psillakis, Enhancement of biodegradability of industrial wastewaters by chemical oxidation pre-treatment, *J. Chem. Technol. Biotechnol.* 79 (2004) 431–454.
- [29] I. Oller, S. Malato, J.A. Sánchez-Pérez, W. Gernjak, M.I. Maldonado, L.A. Pérez-Estrada, C. Pulgarín, Reduction in residual COD in biologically treated paper mill effluents by means of combined ozone and ozone/UV reactor stages, *Catal. Today* 122 (2007) 150–159.
- [30] V. Kavitha, K. Palanivelu, The role of ferrous ion in Fenton and photo-Fenton processes for the degradation of phenol, *Chemosphere* 55 (2004) 1235–1243.
- [31] J.A. Zazo, J.A. Casas, A.F. Mohedano, M.A. Gilarranz, J.J. Rodríguez, Chemical pathway and kinetics of phenol oxidation by Fenton's reagent, *Environ. Sci. Technol.* 39 (2005) 9295–9302.
- [32] D. Hermosilla, M. Cortijo, C.P. Huang, The role of iron on the degradation and mineralization of organic compounds using conventional Fenton and photo-Fenton processes, *Chem. Eng. J.* 155 (2009) 637–646.
- [33] M.S. Yalfani, S. Contreras, F. Medina, J. Sueiras, Phenol degradation by Fenton's process using catalytic in situ generated hydrogen peroxide, *Appl. Catal. B* 89 (2009) 519–526.
- [34] R.F.F. Pontes, J.E.F. Moraes, A. Machulek Jr., J.M. Pinto, A mechanistic kinetic model for phenol degradation by the Fenton process, *J. Hazard. Mater.* 176 (2010) 402–413.
- [35] APHA, AWWA, WPCF (Eds.), *Standard methods for the examination of water and wastewater*, Washington DC, 1989.
- [36] H. Pobiner, Determination of hydroperoxides in hydrocarbon by conversion to hydrogen peroxide and measurement by titanium complexing, *Anal. Chem.* 33 (1961) 1423–1428.
- [37] D. Hermosilla, M. Cortijo, C.P. Huang, Optimizing the treatment of landfill leachate by conventional Fenton and photo-Fenton processes, *Sci. Total Environ.* 407 (2009) 3473–3481.
- [38] S.E. Manahan, *Environmental Chemistry*, CRC Press, Boca Ratón, 2010.
- [39] V. Kavitha, K. Palanivelu, Degradation of 2-chlorophenol by Fenton and photo-Fenton processes—a comparative study, *J. Environ. Sci. Health A* 38 (2003) 1215–1231.
- [40] H. Kusic, N. Koprivanac, A.L. Bozic, Photo-assisted Fenton type processes for the degradation of phenol: a kinetic study, *Chem. Eng. J.* 123 (2006) 127–137.
- [41] M.D. Zeyaulah, A.S. Abdelkaf, W.B. Zabya, A. Ali, Biodegradation of catechols by micro-organisms – a short review, *Afr. J. Biotechnol.* 8 (2009) 2916–2922.
- [42] L. Pramparo, M.E. Suárez-Ojeda, J. Pérez, J. Carrera, Kinetics of aerobic biodegradation of dihydroxybenzenes by a *p*-nitrophenol-degrading activated sludge, *Bioresour. Technol.* 110 (2012) 57–62.
- [43] D. Hermosilla, N. Merayo, R. Ordóñez, A. Blanco, Optimization of conventional Fenton and ultraviolet-assisted oxidation processes for the treatment of reverse osmosis retentate from a paper mill, *Waste Manage.* 32 (2012) 1236–1243.
- [44] S. Kim, A. Vogelpohl, Degradation of organic pollutants by the photo-Fenton-process, *Chem. Eng. Technol.* 21 (1998) 187–191.
- [45] M.I. Stefan, J.R. Bolton, Mechanism of the degradation of 1,4-dioxane in dilute aqueous solution using the UV/hydrogen peroxide process, *Environ. Sci. Technol.* 32 (1998) 1588–1595.
- [46] I.R. Moraes, F.C. Nart, Sulfate ions adsorbed on Au(hkl) electrodes: in situ vibrational spectroscopy, *J. Electroanal. Chem.* 461 (1999) 110–120.
- [47] Y.M. Jung, Characterization of pH-dependent IR spectra of oxalic acid: comparison of self-modeling curve resolution analysis with calculation of IR frequencies, *Bull. Korean Chem. Soc.* 24 (9) (2003) 1410–1412.
- [48] B. Jin, P. Liu, Y. Wang, Z. Zhang, Y. Tian, J. Yang, S. Zhang, F. Cheng, Rapid-scan time-resolved FT-IR spectroelectrochemistry studies on the electrochemical redox process, *J. Phys. Chem. B* 111 (2007) 1517–1522.
- [49] J. Araña, J.M. Doña Rodríguez, O. González Díaz, J.A. Herrera Medián, C. Fernández Rodríguez, J. Pérez Peña, The effect of acetic acid on the photocatalytic degradation of catechol and resorcinol, *Appl. Catal. A Gen.* 299 (2006) 274–284.
- [50] H. Gulley-Stahl, P.A. Hogan II, W.L. Schmidt, S.J. Wall, A. Buhrlage, A.A. Bullen, Surface complexation of catechol to metal oxides: an ATR-FTIR, adsorption, and dissolution study, *Environ. Sci. Technol.* 44 (2010) 4116–4121.
- [51] F.C. Nart, T. Iwasita, M. Weber, Sulfate adsorption on well-define Pt (100) electrodes, *Electrochim. Acta* 39 (13) (1994) 2093–2096.
- [52] R.T.S. Muthu Lakshmi, M.K. Vyas, A.S. Brar, I.K. Varma, Synthesis and characterization of sulphonated PEES copolymers by NMR spectroscopy, *Eur. Polym. J.* 42 (2006) 1423–1432.
- [53] M.M. Hasani-Sadrabadi, S.H. Emami, H. Moaddel, Preparation and characterization of nanocomposite membranes made of poly(2,6-dimethyl-1,4-phenylene oxide) and montmorillonite for direct methanol fuel cells, *J. Power Sources* 183 (2008) 551–556.